

Mitochondrial Complex I Inhibitor Rotenone Induces Apoptosis through Enhancing Mitochondrial Reactive Oxygen Species Production*

Received for publication, October 11, 2002, and in revised form, December 12, 2002
Published, JBC Papers in Press, December 20, 2002, DOI 10.1074/jbc.M210432200

Nianyu Li‡, Kathy Ragheb‡, Gretchen Lawler‡, Jennie Sturgis‡, Bartek Rajwa‡, J. Andres Melendez§, and J. Paul Robinson‡¶

From the ‡Purdue University Cytometry Laboratories, Department of Basic Medical Sciences, Purdue University, West Lafayette, Indiana 47907 and the §Center for Immunology & Microbial Disease, MC-151, Albany Medical College, Albany, New York 12208

Inhibition of mitochondrial respiratory chain complex I by rotenone had been found to induce cell death in a variety of cells. However, the mechanism is still elusive. Because reactive oxygen species (ROS) play an important role in apoptosis and inhibition of mitochondrial respiratory chain complex I by rotenone was thought to be able to elevate mitochondrial ROS production, we investigated the relationship between rotenone-induced apoptosis and mitochondrial reactive oxygen species. Rotenone was able to induce mitochondrial complex I substrate-supported mitochondrial ROS production both in isolated mitochondria from HL-60 cells as well as in cultured cells. Rotenone-induced apoptosis was confirmed by DNA fragmentation, cytochrome *c* release, and caspase 3 activity. A quantitative correlation between rotenone-induced apoptosis and rotenone-induced mitochondrial ROS production was identified. Rotenone-induced apoptosis was inhibited by treatment with antioxidants (glutathione, *N*-acetylcysteine, and vitamin C). The role of rotenone-induced mitochondrial ROS in apoptosis was also confirmed by the finding that HT1080 cells overexpressing magnesium superoxide dismutase were more resistant to rotenone-induced apoptosis than control cells. These results suggest that rotenone is able to induce apoptosis via enhancing the amount of mitochondrial reactive oxygen species production.

The mitochondrial respiratory chain (complexes I–V) is the major site of ATP production in eukaryotes. Recently it was recognized that this organelle not only generates ATP, but also plays an important role in apoptosis (for reviews see Refs. 1–3).

It is now clear that upon apoptotic stimulation mitochondria can release several proapoptotic regulators, including cytochrome *c* (4), Smac/Diablo (5, 6), endonuclease G (7), and apoptosis-inducing factor (8), to the cytosol. These proapoptotic regulators will then activate cellular apoptotic programs downstream (for reviews see Refs. 1–3). The release of proapoptotic regulators is further regulated by the translocation of Bcl-2 family proteins (9, 10). Although this evidence places mitochondria in the center of the apoptotic signaling pathway, the role of

mitochondrial respiratory chain activity in apoptosis is still elusive.

Inhibition of the mitochondrial respiratory chain by rotenone has been widely used to study the role of the mitochondrial respiratory chain in apoptosis (11–13). Some recent evidence showed that rotenone, a mitochondrial respiratory chain complex I inhibitor, could induce cell death in a variety of cells (11–16). The importance of mitochondrial respiratory chain complex I inhibitor-induced apoptosis was further recognized with the finding that tumor necrosis factor (TNF)- α could inhibit the mitochondrial respiratory chain at the mitochondrial complex I site (14). However, contradictory reports showed that rotenone could inhibit apoptosis in other systems (17–19).

It has been suggested that ROS¹ play an important role in apoptosis, and several groups have shown that molecules that stimulate formation of ROS can result in apoptosis (20, 21) and a process inhibited by antioxidants (22, 23). Others reported production of ROS by a wide range of apoptotic stimuli, including TNF, ceramide, staurosporine, and UV radiation (24–27). The mitochondrial respiratory chain is one of the most important sites of ROS production under physiological conditions (28–30), and it has been long suspected that mitochondrial ROS play an important role in apoptosis. The mitochondrial-derived ROS are vital not only because mitochondrial respiratory chain components are present in almost all eukaryotic cells, but also because the ROS produced in mitochondria can readily influence mitochondrial function without having to cope with long diffusion times from the cytosol. Two sites in the respiratory chain, complex I and complex III, have been suggested to be the major ROS source (31–33). Based on stoichiometrical calculation, superoxide was suggested as the primary product, with hydrogen peroxide as the secondary product (34). Mitochondrial-derived ROS could be modified when the mitochondrial respiratory chain was interrupted under pathological conditions or by respiratory chain inhibitors (31, 33). Early reports showed that the complex I inhibitor rotenone and the complex b-c1 inhibitor antimycin could stimulate superoxide and hydrogen peroxide formation on submitochondrial particles (31, 35). However, results of rotenone-induced mitochondrial ROS production measured at the cellular level appeared inconsistent with conflicting results reporting that rotenone could elevate cellular ROS production in some cases (11, 36)

* The costs of publication of this article were defrayed in part by the payment of page charges. This article must therefore be hereby marked "advertisement" in accordance with 18 U.S.C. Section 1734 solely to indicate this fact.

¶ To whom correspondence should be addressed: Purdue University Cytometry Laboratories, Dept. of Basic Medical Sciences, Purdue University, West Lafayette, IN 47907. Tel.: 765-494-0757; Fax: 765-494-0517; E-mail: jpr@flowcyt.cyto.purdue.edu.

¹ The abbreviations used are: ROS, reactive oxygen species; PHPA, *p*-hydroxyphenylacetate; Mn-SOD, manganese superoxide dismutase; HE, hydroethidium; EB, ethidium bromide; NAC, *N*-acetylcysteine; PI, propidium iodide; Tiron, 4,5-dihydroxy-1,3-benzene-disulfonic acid; PBS, phosphate-buffered saline; HBSS, Hank's balanced salt solution; Me₂SO, dimethyl sulfoxide; Z, benzyloxycarbonyl.

while inhibiting cellular ROS production in others (17, 37, 38).

The present investigation studied the mechanism of rotenone-induced apoptosis. Our data show that rotenone can induce mitochondrial ROS production and that rotenone-induced mitochondrial ROS production is closely related to rotenone-induced apoptosis.

MATERIALS AND METHODS

Cell Culture and Reagents—Hoechst 33342, propidium iodide (PI), and anti-cytochrome oxidase subunit VI antibody were obtained from Molecular Probes, Eugene, OR. Hydroethidine was obtained from Polysciences, Warrington, PA. Anti-human caspase 3 antibody and anti-human cytochrome *c* antibody were obtained from Santa Cruz Biotechnology, Inc., Santa Cruz, CA. All other reagents, unless otherwise stated, were obtained from Sigma Chemical Co.

The human promyelocytic leukemia cell line HL-60 was obtained from ATCC (Manassas, VA). Cells were cultured in RPMI 1640 medium supplemented with 10% fetal calf serum and 2 mM L-glutamine.

HL-60 cells lacking mitochondrial DNA (ρ^0) were generated by growing HL-60 cells in RPMI 1640 medium supplied with 10% fetal calf serum, 2 mM L-glutamine, 1 mM pyruvate, 50 μ g/ml uridine, 25 mM glucose, and 50 ng/ml ethidium bromide for 8 weeks as previously described (39). After selection, the cells were grown in the same medium without ethidium bromide. Oxygen consumption was measured with a Clark-type oxygen electrode, and no oxygen uptake was observed for ρ^0 HL-60 cells.

The human fibrosarcoma cell line HT-1080 was maintained in Dulbecco's modified Eagle's medium containing 10% heat-inactivated fetal calf serum and supplemented with 2 mM L-glutamine, 1 mM sodium pyruvate, and 100 units/ml penicillin. Construction of a stable HT1080 cell line overexpressing magnesium superoxide dismutase (Mn-SOD) was previously described in detail (40). HT1080 cells stably transfected with Mn-SOD were maintained in medium that included 1 mg/ml G418 in addition to the above-mentioned supplements. All cell lines were cultured at 37 °C with 5% CO₂.

Respiration Measurement—Oxygen consumption was measured with a Clark oxygen electrode (model 5300; Yellow Spring Instrument Co., Yellow Spring, OH) as described before (41). Briefly, 1×10^7 HL-60 cells were treated with various concentrations of rotenone for 30 min. Cells were then collected and resuspended in a medium containing 0.3 M mannitol, 10 mM potassium HEPES (pH 7.4), 5 mM potassium phosphate (pH 7.4), and 1 mM MgCl₂. The cells were injected into a respiration chamber that was then sealed. The total volume of the respiration chamber was 1.6 ml. Respiration was then measured and calculated as the rate of change in the oxygen concentration, assuming the initial oxygen concentration to be 6.8 mg/liter. Cell respiration was converted to percentage of control.

ATP Determination—For ATP measurement, a commercially available luciferin-luciferase assay kit was used. Briefly, HL-60 cells were treated with various concentrations of rotenone for 24 h and then collected in 1-ml Eppendorf tubes. After a single wash with ice-cold PBS, cells were lysed with the somatic cell ATP-releasing reagent provided by the kit. Luciferin substrate and luciferase enzyme were added and bioluminescence was assessed on a Perkin Elmer 3B spectrofluorometer. Whole-cell ATP content was determined by running an internal standard. The cellular ATP level was converted to percentage of untreated cells (control).

Measurement of Hydrogen Peroxide Production by Intact Mitochondria—Intact mitochondria were isolated from cultured HL-60 cells. HL-60 cells (1×10^9 cells) were collected by centrifugation at $500 \times g$ for 5 min. After one wash with ice-cold Ca²⁺, Mg²⁺-free PBS at $250 \times g$, the cells were resuspended in 2 ml of isolation buffer containing 250 mM sucrose, 10 mM HEPES (pH 7.4), and 1 mM EDTA. Cells were homogenized in an ice-cold Dounce homogenizer with 20 strokes. Cell disruption was confirmed by trypan blue staining. The disrupted cells were centrifuged for 10 min at $600 \times g$ at 4 °C. Supernatant was collected and centrifuged at $15,000 \times g$, 4 °C, for 10 min, and the resulting pellet was considered as crude mitochondria. The crude mitochondria were further washed twice with the same isolation buffer as described above. The resulting mitochondria pellet was resuspended in isolation buffer without EDTA. Mitochondria suspensions were kept on ice, and all experiments were performed within 5 h. Mitochondrial protein concentration was determined by the biuret method (Bio-Rad) with bovine serum albumin as the standard.

Mitochondrial hydrogen peroxide production was measured from the increase of oxidized *p*-hydroxyphenylacetate (PHPA) fluorescence by horseradish peroxidase (41, 43). Fluorescence of oxidized PHPA (excitation 320 nm, emission 400 nm) was measured by a Perkin Elmer 3B spectrofluorimeter. Mitochondria (0.5 mg of protein) were added to 4 ml of medium containing 0.3 M mannitol, 10 mM potassium HEPES (pH 7.4), 5 mM potassium phosphate (pH 7.4), 1 mM MgCl₂, 10 μ g/ml PHPA, 10 units of horseradish peroxidase, and the substrates for various mitochondrial respiratory chain complexes. Mitochondrial hydrogen peroxide production was determined by interpolation from the standard curve generated by reagent hydrogen peroxide.

Measurement of Cellular Superoxide Production by Flow Cytometry—Measurement of cellular superoxide production was performed as described previously, with some modifications (44). For HL-60 cells, cells were treated with various concentrations of rotenone for 30 min. Cells were then collected and washed in Hank's balanced salt solution (HBSS) at $250 \times g$. Cells were resuspended in HBSS containing 10 μ M hydroethidine (HE) and incubated at 37 °C for 10 min. For HT1080 fibrosarcoma cells, cells were treated with rotenone for 30 min, the medium was then removed, and cells were washed once with HBSS. Cells were then incubated HBSS containing 0.25% trypsin for 5 min. Cells were then resuspended in HBSS containing 10 μ M hydroethidine (HE), and incubated at 37 °C for 10 min. All cell suspensions were placed into 12 \times 75-mm tubes for assay. Flow cytometry studies were carried out on a Beckman-Coulter XL flow cytometer. Ethidium fluorescence was collected using a 610-nm long-pass filter.

DNA Fragmentation—The DNA fragmentation assay was performed according to the method described previously with some modifications (45). HL-60 cells were treated with various concentrations of rotenone in the presence or absence of antioxidants. Cells (2×10^7) were washed once with PBS (4 °C, pH 7.4) and collected by centrifugation at $250 \times g$ for 5 min. The pellet was then treated with 0.5 ml of lysis buffer (10 mM Tris-HCl, pH 7.4, 10 mM EDTA, 0.5% sodium dodecyl sulfate) for 10 min on ice. After treatment with RNase A (final concentration, 100 μ g/ml) for 1 h at 37 °C, the cells were incubated at 50 °C for 4 h in the presence of 100 μ g/ml proteinase K. DNA was precipitated by addition of 50 μ l of 3 M sodium acetate (pH 5.2) and 1 ml of cold (4 °C) 100% ethanol to the solution. DNA was then collected and dissolved in TE buffer (10 mM Tris pH 8.0, EDTA 1 mM). For analysis, 10–20 μ l of DNA was loaded on a 1.2% agarose gel containing 10 μ g/ml ethidium bromide. Electrophoresis was performed in 0.5 \times Tris borate-EDTA buffer (18 mM Tris-base (pH 8.0), 18 mM boric acid, and 1 mM EDTA) at 70 V for 2 h. DNA was visualized under ultraviolet light and photographed.

Subcellular Fractionation—For HL-60 cells, 2×10^6 were collected by centrifugation at $250 \times g$ for 5 min. For HT1080 cells, cells were collected by trypsinization and then centrifuged ($250 \times g$) for 5 min. All cells were then resuspended in buffer containing 250 mM sucrose, 10 mM HEPES, and 1 mM EDTA, pH 7.4, 4 °C. Digitonin (400 ng/ml) was then added to the cell suspension and lysis of cells confirmed by examining the entry of trypan blue into the cytosol. The cell suspension was centrifuged at $5,000 \times g$ for 10 s at 4 °C to pellet the unbroken cells. The resulting supernatant was centrifuged at $12,000 \times g$ for 10 min at 4 °C. The final supernatant was considered as the cytosol fraction, and the final pellet was used as the mitochondrial fraction.

Whole Cell Extraction—For HL-60 cells, $\sim 1 \times 10^7$ cells were harvested and washed once with ice-cold PBS, resuspended in 1 ml of ice-cold lysis buffer containing 1% Nonidet P-40, 20 mM Tris-HCl (pH 8.0), 10% glycerol, 137 mM NaCl, 2 mM EDTA, 10 μ g/ml aprotinin, 10 μ g/ml leupeptin, 1 mM phenylmethylsulfonyl fluoride, 1 mM dithiothreitol, and 1 mM sodium orthovanadate, and incubated on ice for 30 min. After centrifugation at $12,000 \times g$ for 10 min at 4 °C, cell lysates were transferred to fresh tubes and stored at -80 °C. For HT1080 cells, cells at 80–90% confluence in 100-mm culture dishes were washed once with HBSS and placed on ice. In each culture dish, 400 μ l of lysis buffer was added. After 10 min of incubation, the solubilized proteins were centrifuged at $12,000 \times g$ in a microcentrifuge (4 °C) for 10 min, and the supernatants were stored at -80 °C.

Western Blotting—Cell homogenates (50 μ g of protein) were fractionated by SDS-PAGE on a 15% acrylamide gel. Bands of proteins were then transferred to a polyvinylidene difluoride (PVDF) membrane (Bio-Rad). The PVDF membrane was blocked by PBS containing 5% milk overnight at 4 °C and then incubated with antibodies against either cytochrome *c*, caspase 3, β -actin, or cytochrome oxidase subunit VI for 3 h at room temperature. After an additional 1-hour incubation with horseradish peroxidase-conjugated secondary antibodies, the binding of antibodies to the PVDF membrane was detected with an enhanced chemiluminescence Western blotting analysis (Amersham Biosciences).

Measurement of Apoptosis by Flow Cytometry and Confocal Microscopy—Degradation of DNA was measured by flow cytometry and confocal microscopy. For flow cytometry analysis, PI was used to detect DNA breakdown as described previously (46). Cells were collected and

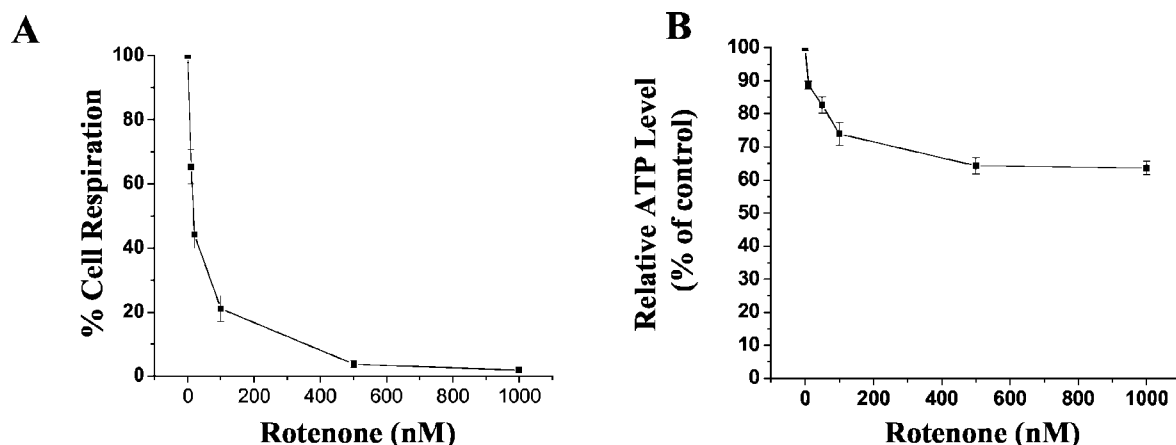
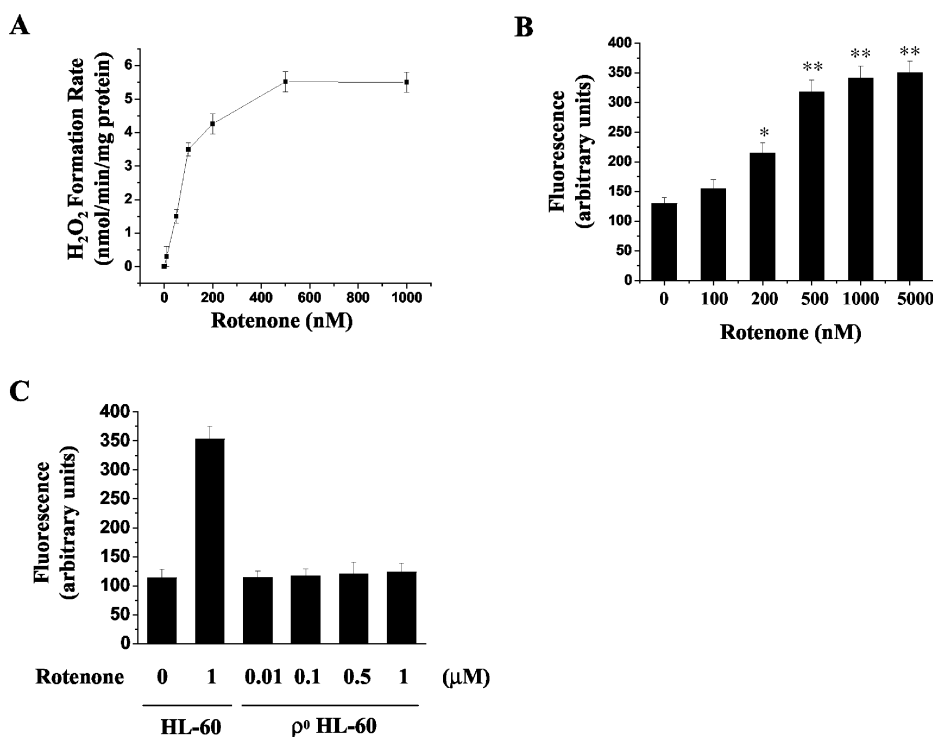


FIG. 1. Inhibitory effects of rotenone on cell respiration and cellular ATP levels. *A*, HL-60 cells were treated with various concentrations of rotenone for 30 min before measurement of cell respiration. Respiration was calculated as percentage of control. *B*, HL-60 cells were treated with rotenone for 24 h and collected for whole cell ATP measurement as described under "Materials and Methods." ATP values are expressed as percent of control. All values are means \pm S.E., $n = 3$.

FIG. 2. Effect of rotenone on ROS production. *A*, mitochondria were isolated from HL-60 cells and incubated with various concentrations of rotenone and glutamate/malate. Hydrogen peroxide produced by mitochondria was measured as described under "Materials and Methods." Mitochondrial hydrogen peroxide was converted to nmol of hydrogen peroxide produced per min per mg of mitochondrial protein. Values are means \pm S.E., $n = 3$. *B*, intact HL-60 cells were treated with various concentrations of rotenone for 30 min. Cells were then collected and loaded with 10 μ M hydroethidine for 10 min. ROS levels were estimated by measuring ethidium fluorescence using flow cytometry. *C*, cellular ROS production in ρ^0 HL-60 cells treated with various concentrations of rotenone for 1 h as indicated.



fixed in suspension in 70% ethanol on ice, and then stored at -20°C for at least 4 h. Cells were washed with 5 ml of HBSS, centrifuged again, and resuspended in 1 ml of HBSS. After addition of 0.2 ml of phosphate citrate buffer (0.2 M Na_2HPO_4 , 4 mM citric acid, pH 7.8), cells were incubated at room temperature for 5 min before being washed again and resuspended in HBSS containing 20 $\mu\text{g/ml}$ PI and 10 $\mu\text{g/ml}$ RNase A. Cells were incubated in the dark at room temperature for 30 min. PI fluorescence was analyzed by flow cytometry.

Apoptosis was also measured by observing morphological changes in the nuclear chromatin of cells detected by staining with 2 $\mu\text{g/ml}$ Hoechst 33342 at room temperature for 15 min, followed by examination on a Bio-Rad MRC 1024 confocal microscope.

RESULTS

Impairment of Mitochondrial Function in HL-60 Cells by Rotenone—Rotenone-induced mitochondrial dysfunction was investigated by both respiration measurement and determination of cellular ATP level. Fig. 1A shows the dose-dependent response of rotenone-inhibited HL-60 cell respiration. Inhibition of cell respiration was detectable at rotenone levels as low as 10 nM. Below 100 nM, increasing concentrations of rotenone

produced a rapid decrease in the respiration of the cells. Above 100 nM, the inhibition of respiration continued, but at a lower rate. Rotenone at 500 nM inhibited cell respiration by over 96%.

The curve of ATP inhibition by rotenone was similar to the respiration curve (Fig. 1B). Increasing concentrations of rotenone below 100 nM result in a sharp decrease of cellular ATP level. Above 100 nM, cellular ATP level still decreased, but at a much slower rate. Rotenone at 500 nM decreased cellular ATP level to 64% of control. Higher concentrations of rotenone did not further decrease the ATP level. By comparison, 10 μM oligomycin inhibited cellular ATP level to 55% of control (data not shown).

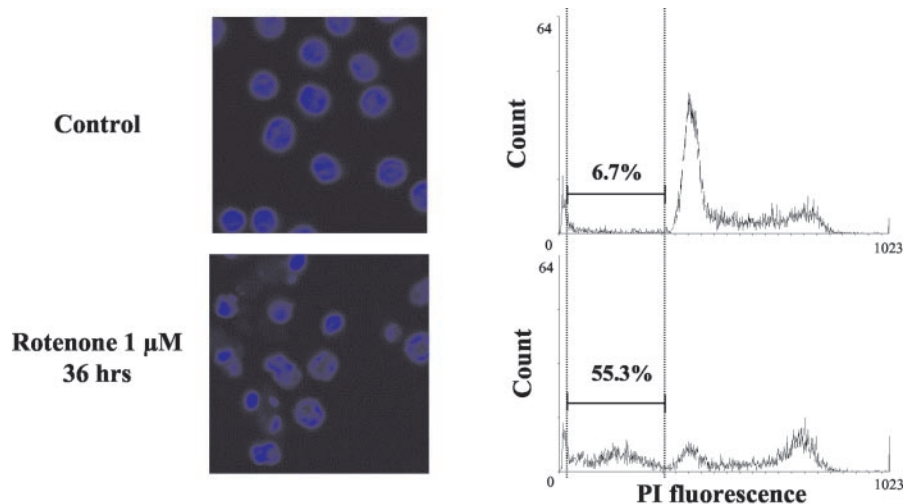
Generation of Mitochondrial ROS by Rotenone in HL-60 Cells—Production of mitochondrial reactive oxygen species by HL-60 cells was estimated for both isolated mitochondria and cultured cells. For mitochondrial ROS measurement, a classical horseradish peroxidase-based PHPA oxidation method was used to detect hydrogen peroxide leaked from intact mitochondria when mitochondria were incubated with various respira-

TABLE I
Rotenone-induced mitochondrial hydrogen peroxide production

Mitochondria were isolated from HL-60 cells and incubated with various respiratory chain substrates and inhibitors. Hydrogen peroxide produced by mitochondria was measured as described under "Materials and Methods." Mitochondrial hydrogen peroxide was converted to nmol of hydrogen peroxide produced per min per mg of mitochondrial protein. Values are means \pm S.E., $n = 3$.

Substrate	Inhibitor	Rate of H ₂ O ₂ production nmol/min/mg protein
Glutamate (5 mM) + malate (5 mM)	Rotenone (1 μ M)	0.129 \pm 0.049
Glutamate (5 mM) + malate (5 mM)	Antimycin (1 μ M)	5.524 \pm 0.321
Glutamate (5 mM) + malate (5 mM)		5.563 \pm 0.314
Succinate (5 mM)		0.204 \pm 0.052
Succinate (5 mM)	Rotenone (1 μ M)	0.105 \pm 0.057
Succinate (5 mM)	Antimycin (1 μ M)	14.54 \pm 1.213

FIG. 3. Effect of rotenone on DNA breakdown in HL-60 cells. HL-60 cells were incubated with either Me₂SO (*control*) or 1 μ M rotenone in Me₂SO for 36 h. *Left panel*, cells stained with Hoechst 33342 and imaged on the confocal microscope. *Right panel*, cells fixed and stained with PI as described under "Materials and Methods." The number of apoptotic cells was estimated by gating on the subdiploid population. Cells with extensive DNA breakdown were not considered as apoptotic cells and were gated out. Numbers on each gate show the percentage of apoptotic cells in that *histogram*. Data are representative of three separate flow cytometry analyses.



tory chain substrates and inhibitors. As reported by Hansford *et al.* (42), an inhibition of mitochondrial hydrogen peroxide formation was observed in our system when a higher concentration of PHPA was used. However, the concentration at which we observed inhibition was much lower than that reported by Hansford *et al.* (20 μ g/ml versus 50 μ g/ml). Below 20 μ g/ml, inhibition of hydrogen peroxide formation by PHPA was not observed (data not shown). Therefore, a final concentration of 10 μ g/ml PHPA was selected to be used in the current study.

Mitochondria from HL-60 cells were able to generate a low level of hydrogen peroxide (Fig. 2A and Table I) in the presence of mitochondrial respiratory chain substrates, glutamate/malate for complex I and succinate for complex II. The mitochondrial complex I inhibitor rotenone increased glutamate/malate-supported hydrogen peroxide formation. The concentration of rotenone capable of inducing mitochondrial hydrogen peroxide formation was closely related to the concentration that inhibited cell respiration. At low concentrations, cell respiration levels were highly sensitive to rotenone treatment. The respiration inhibition curve was very rapid with a nearly 80% decrease of cell respiration in the presence of 100 nM rotenone. Similarly, mitochondrial hydrogen peroxide formation increased quickly within the same rotenone concentration range. Respiration in cells treated with 0.5 μ M rotenone was reduced to 4% of control levels. Higher concentrations of rotenone produced greater inhibition but a much slower decrease in cell respiration. Correspondingly, 0.5 μ M rotenone stimulated the maximum rate of mitochondrial hydrogen peroxide production. Higher concentrations of rotenone did not further elevate this rate.

Another mitochondrial respiratory chain inhibitor, antimycin, was also able to stimulate mitochondrial hydrogen peroxide formation (Table I). However, antimycin could elevate both glutamate/malate- and succinate-supported mitochondrial hydrogen peroxide formation, while rotenone was shown to

increase only glutamate/malate-supported hydrogen peroxide formation.

To confirm that rotenone was able to induce mitochondrial ROS production, conversion of the ROS-sensitive dye hydroethidine to ethidium was used to measure cellular ROS level by flow cytometry (Fig. 2B). Using this technique, rotenone-induced ROS production was detected in single cells at the whole-cell level. Rotenone was shown to elevate cellular ROS levels in HL-60 cells. In comparison with the dose-response curve of rotenone-induced mitochondrial hydrogen peroxide formation, at the cellular level low concentrations of rotenone (<100 nM) could merely elevate the cellular ROS level. However, at high concentrations (\geq 500 nM) rotenone could significantly increase the cellular ROS level.

To further investigate whether rotenone-induced cellular superoxide production was from mitochondria, HL-60 cells that lack mitochondrial DNA (ρ^0) were treated with various concentrations of rotenone and then loaded with hydroethidine. Rotenone could not elevate ethidium fluorescence in ρ^0 HL-60 cells after treatment for 1 h (Fig. 2C), although ethidium fluorescence increased when normal HL-60 cells were treated with rotenone for the same length of time (Fig. 2C).

Rotenone-induced Apoptotic Cell Death in HL-60 Cells—Using HL-60 cells as a model, we studied the effect of rotenone on cell death. After treatment with 1 μ M rotenone for 36 h, \sim 50% of the HL-60 cells showed chromatin condensation and nuclear fragmentation under confocal microscopy using Hoechst 33342 as DNA stain (Fig. 3). Cell cycle analysis based on flow cytometry was used to quantitatively estimate rotenone-induced apoptotic cell death. Gating of the subdiploid cell population on a linear scale excluded cells with extensive DNA degradation (typical of necrosis) to distinguish apoptotic cells from necrotic cells (45). Consistent with confocal microscope results, flow cytometry analysis revealed an increase in the subdiploid pop-

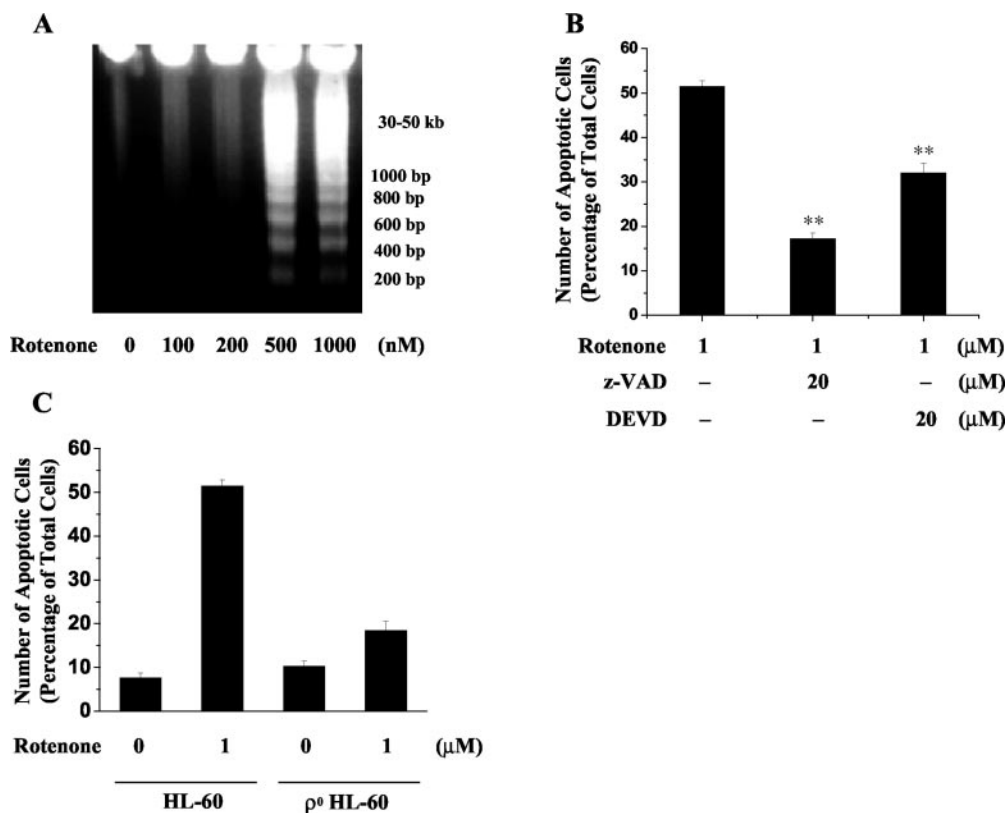


FIG. 4. **Rotenone-induced DNA laddering and effect of caspase inhibitors on rotenone-induced apoptosis.** A, HL-60 cells were treated with different concentrations of rotenone for 36 h. Genomic DNA was isolated and run on a 1% agarose gel and visualized by ethidium bromide staining. Results are representative from three separate experiments. B, cells were pretreated with caspase inhibitors (Z-VAD and DEVD) for 30 min. Rotenone (1 μM) was then added to the medium. After 36 h, cells were collected, and the apoptotic cell number was estimated by flow cytometry as described under "Materials and Methods." Significant difference from control group at *, $p < 0.05$. C, HL-60 cells or ρ^0 HL-60 cells were incubated with either Me₂SO (control) or 1 μM rotenone in Me₂SO for 36 h. Cells were then collected, and the apoptotic cell number was estimated by flow cytometry as described under "Materials and Methods." Significant difference from control group at *, $p < 0.05$.

TABLE II
Rotenone-induced apoptosis in HL-60 cells

HL-60 cells were incubated with either Me₂SO (control) or various concentrations of rotenone in Me₂SO for 36 h. Cells were then fixed and stained with PI as described under "Materials and Methods." The number of apoptotic cells was estimated by gating on the subdiploid population. Cells with extensive DNA breakdown were not considered as apoptotic cells and were gated out. Data were represented as percentage of apoptotic cells in the whole cell population. All values are means \pm S.E., $n = 3$.

Concentration of rotenone	Percentage of apoptotic cells at 36 h
μM	%
0	8.76 \pm 3.309
0.1	15.95 \pm 4.17
0.2	18.15 \pm 1.06
0.5	48.45 \pm 6.15
1	52.8 \pm 3.39
5	53.65 \pm 4.31

ulation after treatment with 1 μM rotenone for 36 h (55.3% compared with 6.7% of control). Agarose gel electrophoresis studies showed that 0.5–1 μM rotenone treatment resulted in a typical apoptotic-style DNA fragmentation with 30/50 kbp and 200/1000 bp oligonucleosomal fragments (Fig. 4A). In addition, the number of subdiploid cells increased in a concentration-dependent manner (Table II). Rotenone (0.5 μM) for 36 h induced ~50% of cells to be subdiploid. Higher concentrations of rotenone did not produce more subdiploid cells than were induced by 0.5 μM rotenone (Table II).

The effects of two caspase inhibitors, the broad caspase inhibitor z-VAD and the specific caspase 3 inhibitor DEVD-CHO

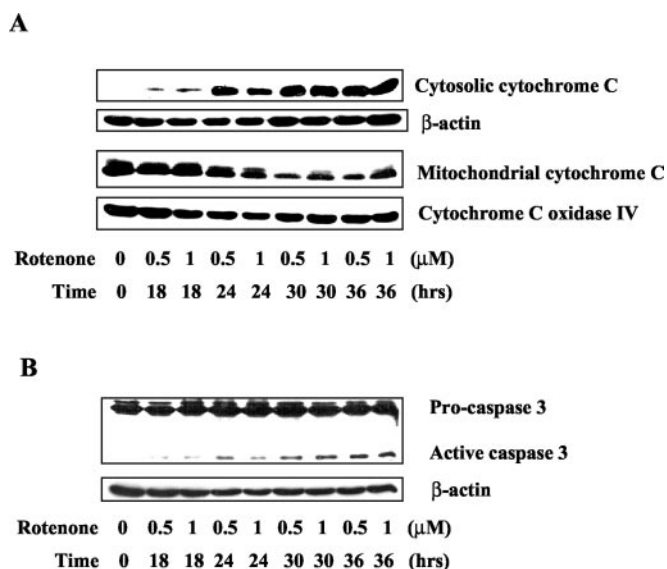


FIG. 5. **Rotenone-induced cytochrome c release and caspase 3 activation in HL-60 cells.** HL-60 cells were treated with rotenone (0.5 or 1 μM) for various times as indicated. A, cytosolic cytochrome c and mitochondrial cytochrome c were determined by immunoblot analyses. B, whole-cell lysate was obtained as described under "Materials and Methods." Caspase 3 activation was determined by immunoblot analysis using caspase 3 antibody to detect both pro-caspase 3 and active caspase 3. β-Actin level was used to confirm the equal loading of samples.

(Bachem, King of Prussia, PA), on rotenone-induced apoptosis were studied (Fig. 4B). Both reagents significantly inhibited rotenone-induced apoptosis, suggesting the involvement of

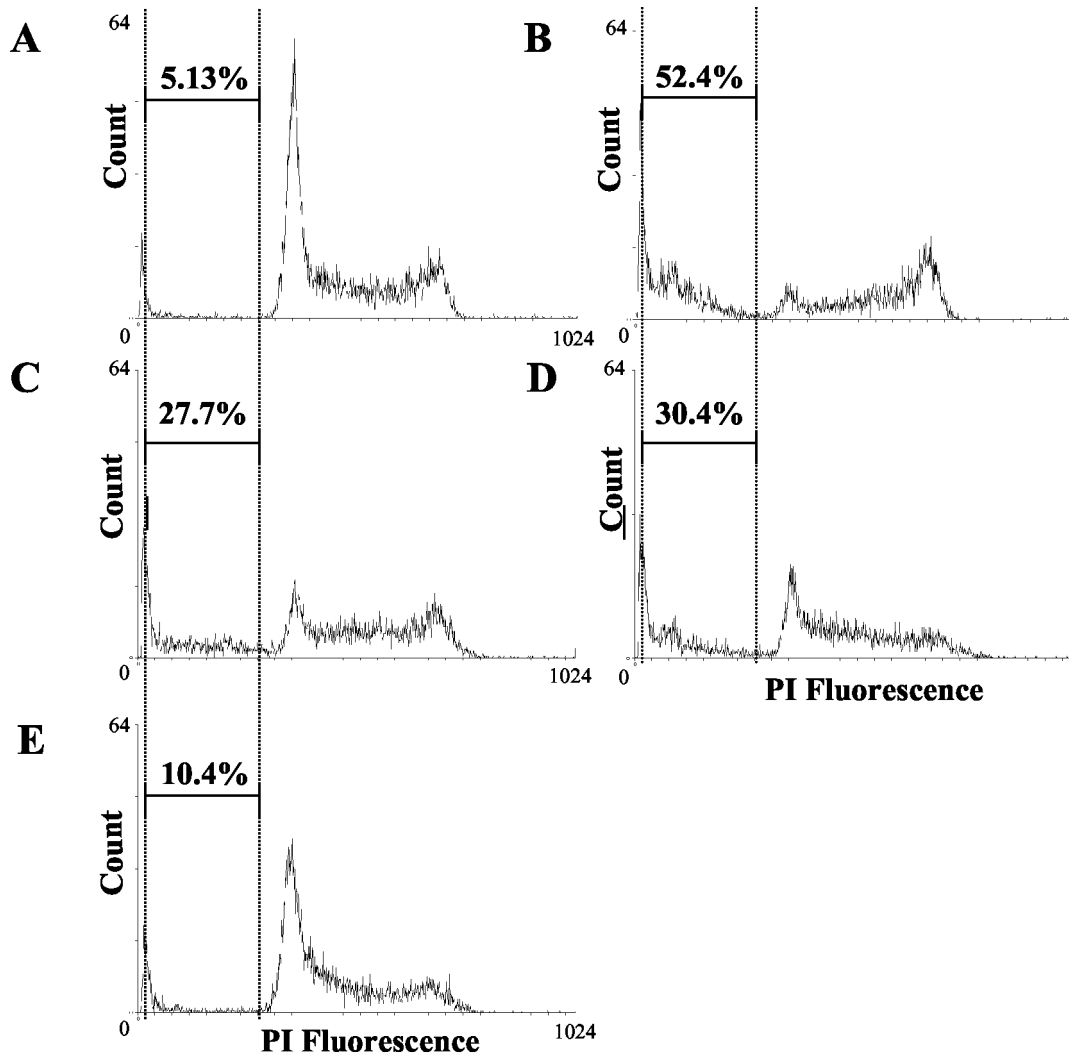


FIG. 6. Inhibition of rotenone-induced DNA breakdown by antioxidants. HL-60 cells were pretreated with either 15 mM glutathione, 15 mM *N*-acetylcysteine, or 15 mM vitamin C for 30 min. Either Me₂SO (control) or 1 μM rotenone in Me₂SO was added to the medium. After 36 h, cells were collected and apoptosis was detected by flow cytometry as described under “Materials and Methods.” Numbers on each gate show the number of apoptotic cells in that histogram. Each histogram is representative of three separate experiments. From top to bottom: A, control (with Me₂SO); B, rotenone, 1 μM; C, rotenone, 1 μM with 15 mM glutathione; D, rotenone, 1 μM with 15 mM *N*-acetylcysteine; E, rotenone, 1 μM with 15 mM vitamin C.

caspsases in rotenone-induced apoptosis. In ρ^0 HL-60 cells, rotenone treatment could cause only around 20% of cells to be apoptotic, much less than the apoptotic cells in normal HL-60 cells (around 52%). We then examined the biochemical properties of rotenone-induced apoptosis. Release of cytochrome *c* from mitochondria to the cytosol and subsequently activation of caspase 3 were considered as the biochemical hallmarks of apoptosis. Western blotting results revealed that after 18 h of rotenone (0.5–1 μM) treatment, mitochondrial cytochrome *c* decreased while cytosol cytochrome *c* increased, indicating a typical release of cytochrome *c* from mitochondria to the cytosol (Fig. 5A). The amount of cytochrome *c* released to the cytosol increased in a time-dependent manner. After a 30-hour treatment, cytochrome *c* release reached a plateau, and no further increase of cytochrome *c* release was observed. Caspase 3 activation was also investigated (Fig. 5B). Caspase 3 was activated at nearly the same time as cytochrome *c* release. Similarly, after rotenone treatment for 18 h, cleavage of pro-caspase 3 to release active caspase was observed. Maximum caspase 3 activation occurred after 30 h.

Inhibition of Rotenone-induced Apoptotic Cell Death by Antioxidants—To study the role of rotenone-induced production of

mitochondrial reactive oxygen species in apoptosis, the effects of antioxidants on rotenone-induced apoptosis were examined. Three classical antioxidants, glutathione, NAC, and vitamin C, were used in the current investigation. All three antioxidants decreased the number of subdiploid cells induced by rotenone treatment at concentrations that are commonly used in other studies (Figs. 6 and 7). Among these antioxidants, vitamin C was shown to be the most potent. Rotenone-induced apoptosis was almost completely inhibited by vitamin C (Figs. 6E and 7A). DNA laddering produced by rotenone treatment was also inhibited by the addition of antioxidants (Fig. 7B), confirming the inhibition of rotenone-induced DNA breakdown by these antioxidants.

Both cytochrome *c* release and caspase 3 activation were found to be inhibited by all three antioxidants (Fig. 8). Similarly, vitamin C was shown to be the most potent among the three. Treatment of cells with 15 mM vitamin C blocked cytochrome *c* release and caspase 3 activation almost entirely (Fig. 8).

Inhibition of Rotenone-induced Cell Death by Mn-SOD Overexpression—To confirm that mitochondrial reactive oxygen species play an important role in rotenone-induced apoptosis, an

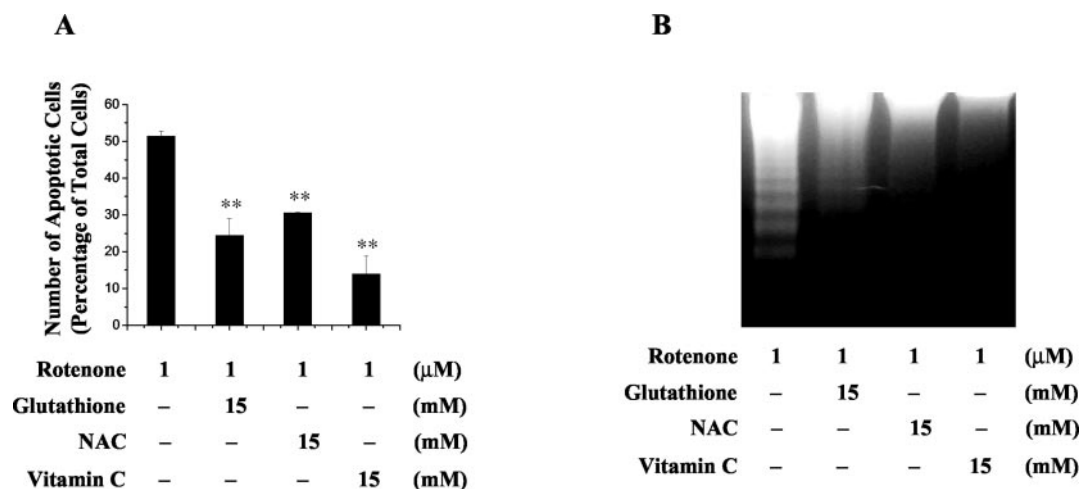


FIG. 7. **Inhibition of rotenone-induced DNA breakdown and DNA laddering by antioxidants.** HL-60 cells were treated with either 15 mM glutathione, 15 mM *N*-acetylcysteine, or 15 mM vitamin C for 30 min. Either Me_2SO (*control*) or 1 μM rotenone in Me_2SO was added to the medium. *A*, after 36 h, cells were collected, and apoptosis was detected by flow cytometry. Data represent percentage of apoptotic cells in the whole cell population. Data are means \pm S.E., $n = 3$. *B*, after 36 h, cells were also collected and genomic DNA was isolated and run on a 1% agarose gel and visualized by ethidium bromide staining. Results are representative from three separate experiments.

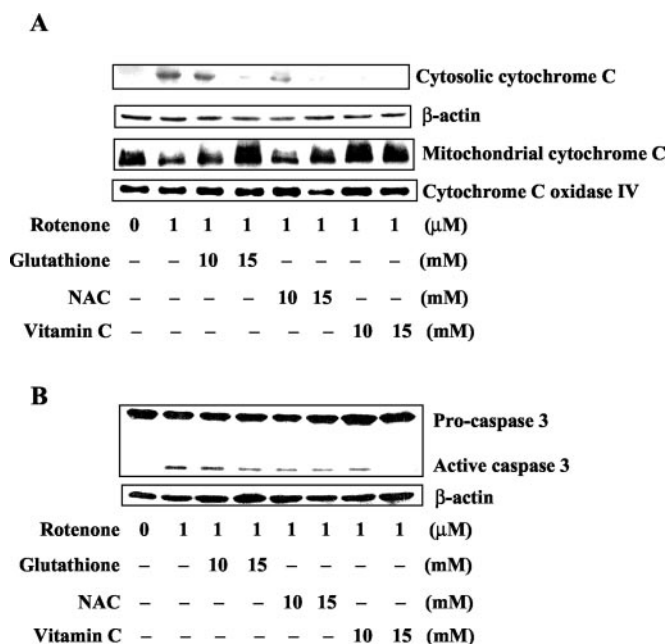


FIG. 8. **Inhibition of rotenone-induced cytochrome *c* release and caspase 3 activation by antioxidants.** HL-60 cells were treated with either glutathione, *N*-acetylcysteine, or vitamin C for 30 min. Either Me_2SO (*control*) or 1 μM rotenone in Me_2SO was added to the medium. After 36 h, cells were collected. *A*, cytosolic cytochrome *c* and mitochondrial cytochrome *c* were determined by immunoblot analyses. *B*, whole-cell lysate was obtained as described under "Materials and Methods." Caspase 3 activation was determined by immunoblot analysis using caspase 3 antibody to detect both pro-caspase 3 and active caspase 3. β -Actin level was used to confirm the equal loading of samples.

Mn-SOD-overexpression cell model was constructed using HT1080 fibrosarcoma cell lines. Two cell lines, CMV (representing HT1080 cells transfected with empty vector) and HT15 (representing HT1080 cells transfected with vector containing Mn-SOD, 15-fold increase in Mn-SOD levels after transfection), were used in the current study. Cellular ROS levels were examined by flow cytometry using hydroethidine as the ROS indicator (Fig. 9A). Basal ethidium fluorescence of HT15 cells was lower than that of CMV cells. Both CMV and HT15 cells showed increase in ethidium fluorescence after 1 μM rotenone

treatment for 30 min, showing that rotenone elevated cellular ROS level in both cell lines. However, the increase of ethidium fluorescence in HT15 cells was about 50% lower than that in CMV cells.

The effects of rotenone on cytochrome *c* release and caspase 3 activation were also studied in both cell lines. Fig. 9B shows the release of cytochrome *c* after rotenone treatment. CMV cells and HT15 cells showed similar basal cytochrome *c* expression in mitochondria. Upon treatment with 1 μM rotenone for 24 h, a great portion of the mitochondrial cytochrome *c* of CMV cells was released from mitochondria to the cytosol. However, mitochondrial cytochrome *c* was largely maintained in mitochondria of HT15 cells. Overexpression of Mn-SOD also inhibited rotenone-induced caspase 3 activation on HT1080 cells. Fig. 9C indicates that after rotenone treatment for 24 h, pro-caspase 3 was largely cleaved in CMV cells. However, in HT15 cells the cleavage of pro-caspase 3 was much less.

Cell cycle analysis by flow cytometry was used to quantitatively estimate the number of apoptotic cells after rotenone treatment in both cell lines. Both untreated CMV and HT1080 cells showed a typical $\text{G}_1\text{S}/\text{G}_2\text{M}$ distribution on flow cytometry (Fig. 10, A and B). After treatment with rotenone (1 μM) for 24 h, more than 50% of CMV cells moved to the subdiploid area, which is typical for apoptotic cells. However, only 20% of the HT15 cells were in the subdiploid area (Fig. 10, C and D).

DISCUSSION

In this study we demonstrated that the ability of the mitochondrial respiratory chain complex I inhibitor rotenone to induce programmed cell death is closely related to its ability to induce mitochondrial ROS production. Previously, rotenone had been reported to enhance glutamate/malate-supported mitochondrial reactive oxygen species production on both bovine heart submitochondrial particles and rat heart intact mitochondria (31, 42). Our result confirmed that in isolated HL-60 cell mitochondria, rotenone induced mitochondrial ROS production through a similar mechanism. The induction of mitochondrial ROS production by rotenone had frequently been attributed to the ability of rotenone to block mitochondrial respiratory chain complex I, thereby increasing the formation of ubiquinone, the primary electron donor in mitochondrial superoxide generation. This also appeared to be the case for HL-60 mitochondria because the concentrations of rotenone that induced mitochondrial ROS corresponded to the concen-

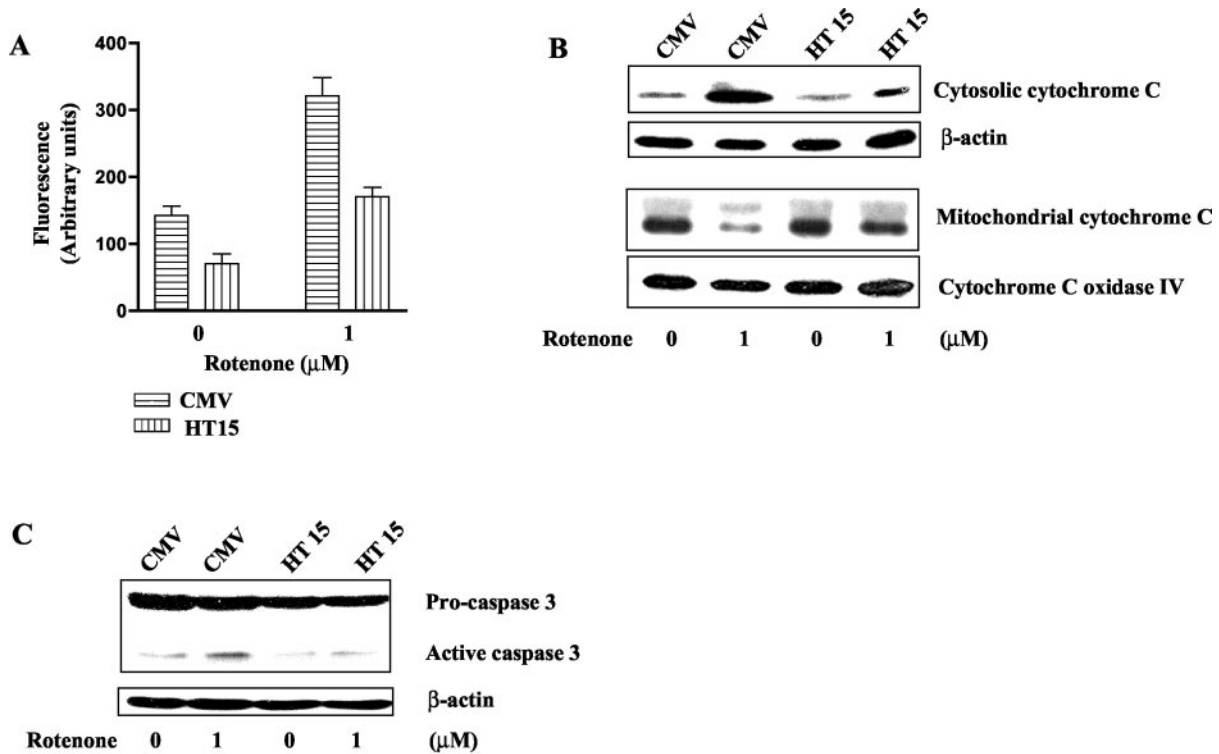
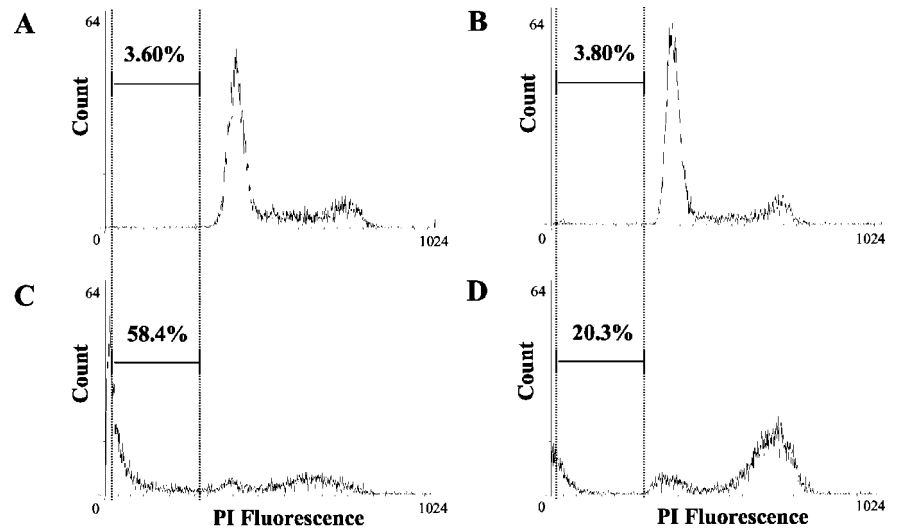


FIG. 9. Effect of Mn-SOD overexpression on rotenone-induced ROS production, cytochrome *c* release, and caspase activation. *A*, control HT1080 cells (CMV) and HL-60 cells overexpressing Mn-SOD (HT15 = 15-fold elevation of Mn-SOD level) were treated with 1 μM rotenone for 30 min. Cells were then loaded with 10 μM hydroethidine. Cellular ROS levels were estimated by measuring ethidium fluorescence using flow cytometry. *B*, CMV and HT15 cells were treated with either Me₂SO or 1 μM rotenone in Me₂SO for 36 h. Cytosolic cytochrome *c* and mitochondrial cytochrome *c* were determined by immunoblot analyses. *C*, caspase 3 activation was determined by immunoblot analysis by caspase 3 antibody to detect both pro-caspase 3 and active caspase 3. β-Actin level was used to confirm the equal loading of samples.

FIG. 10. Effect of Mn-SOD overexpression on rotenone-induced apoptosis. CMV and HT15 cells were treated with either Me₂SO or 1 μM rotenone in Me₂SO for 36 h and then collected. Apoptosis was detected by PI staining using flow cytometry. Numbers on each gate represent the number of apoptotic cells in that histogram. Each histogram is representative of three separate experiments. From top to bottom: *A*, CMV control (with Me₂SO); *B*, HT 15 control (with Me₂SO); *C*, CMV with 1 μM rotenone treatment; *D*, HT 15 with 1 μM rotenone treatment.



trations of rotenone that inhibited cell respiration. In addition, rotenone at 0.5–1 μM resulted in a maximum decrease of cellular ATP level (~63% of control). The respiratory uncoupler oligomycin, which shuts down electron input from both complex I and complex II, resulted in only 8% more inhibition on cellular ATP level (~55% of control), indicating mitochondrial complex I substrates are the major substrates for the mitochondrial respiratory chain in HL-60 cells. For HL-60 cells, these results suggest that once rotenone inhibited mitochondrial respiratory chain complex I, the accumulation of pyruvate/malate in the mitochondria could create a condition that may well be similar to the isolated mitochondrial model.

The whole-cell-level ROS measurement by flow cytometry using hydroethidine confirmed our findings on isolated mito-

chondria. Rotenone induced cellular ROS production dose-dependently. Rotenone could not induce cellular ROS production on ρ⁰ HL-60 cells, further confirming that rotenone-induced cellular ROS originated from mitochondria. At the cellular level, rotenone could enhance cellular ROS level in a similar pattern through a slightly different mechanism. Similar to the results from isolated mitochondria, increasing concentrations of rotenone greater than 0.5 μM produced further but much slower increases in cellular ROS production. However, at lower concentration (100 nM), rotenone was able to increase cellular ROS level only slightly, whereas in the isolated mitochondria model, this concentration could induce a mitochondrial ROS production with close to 50% of maximum ROS production (for rotenone at 1 μM). The possible explanation is that at the

cellular level, the cellular antioxidant system may have a greater impact on the decrease of ROS production.

Rotenone has been reported to cause cell death in a variety of cell lines (11–16). However, whether this cytotoxicity leads to apoptosis or necrosis may depend upon cell type. Our results showed that in HL-60 cells rotenone induced cell death through an apoptotic mechanism. Cell cycle analysis showed a typical apoptotic subdiploid population after rotenone treatment. Chromatin condensation and DNA breakdown were also clearly observable by confocal microscopy. DNA laddering presented as a typical apoptotic DNA cleavage into 50 kbp and 200/1000 bp oligonucleosomal fragments. In addition, Western blots identified release of cytochrome *c* from the mitochondrial compartment to the cytosol after 0.5–1 μ M rotenone treatment. Caspase 3 activation was also demonstrated. All these data indicated that in HL-60 cells rotenone-induced cell death occurs mainly via an apoptotic mechanism as opposed to necrosis. A possible mechanism might be that rotenone inhibits the mitochondrial respiratory chain at the complex I site, decreasing the cellular ATP level; however, the dependence of pyruvate/malate-supported ATP production varies in different cell types. It has already been well established that ATP can act as a switch between apoptosis and necrosis (47–49). A depleted cellular ATP level (usually to around 30% of control) has been shown to inhibit apoptosis (47–49). Therefore, in cell lines highly dependent on pyruvate/malate-supported ATP production, rotenone treatment might drastically decrease the cellular ATP level, which could switch cell death from apoptotic to necrotic. However, this is not the case in HL-60 cells, in which rotenone decreased cellular ATP to a moderate level (63%). Both our results and other reports show that even oligomycin decreases the cellular ATP level in HL-60 cells to around 50–60% of control after 24 h treatment (50). In several other cell lines, such as Jurkat, HeLa, or thymocyte, the same concentrations of oligomycin can decrease the cellular ATP level to less than 20% of control level (47–49). While unlikely to be responsible for these results, the possible impact of high concentrations of rotenone on cellular glycolytic pathways has not been entirely excluded.

Our results strongly suggest that in HL-60 cells, induction of mitochondrial ROS could well be the most significant mechanism of rotenone-induced apoptosis. The concentrations of rotenone that induced apoptosis were in the same range as the concentrations that induced mitochondrial ROS production. Rotenone-induced apoptotic cells in ρ^0 HL-60 cells were much fewer than those in normal HL-60 cells. Several antioxidants (glutathione, vitamin C, and *N*-acetylcysteine) were shown to inhibit rotenone-induced cytochrome *c* release, caspase 3 activation, and DNA breakdown in HL-60 cells. Induction of mitochondrial ROS by rotenone also occurred very early (<1 h) compared with cytochrome *c* release and caspase 3 activation, suggesting that ROS production is upstream of these apoptotic events.

Results from Mn-SOD-overexpressing HT1080 cells confirmed our conclusion that rotenone induced apoptosis via an induction of mitochondrial ROS production. Mn-SOD is the superoxide dismutase that localizes in mitochondria. Mn-SOD is a primary component of the cellular defense system against oxidative toxicity since superoxide can react with hydrogen peroxide to generate singlet oxygen and hydroxyl radicals, which are more toxic than superoxide and hydrogen peroxide (51). In mitochondria, manganese superoxide dismutase is the major enzyme responsible for converting superoxide to hydrogen peroxide (52–54). Overexpression of Mn-SOD inhibited rotenone-induced increase of cellular ROS, confirming that rotenone-induced cellular ROS production in HT1080 cells was

from mitochondria. Consistent with our findings in HL-60 cells, overexpression of Mn-SOD also inhibited rotenone-induced cytochrome *c* release, caspase 3 activation, and DNA breakdown.

The mechanism of rotenone-induced apoptosis is still elusive, and obscured by the occurrence of several concomitant events, including shutdown of the electron transfer through respiratory chain complex I, decreasing cellular ATP level, increasing mitochondrial ROS production, and decreasing mitochondrial membrane potential. Previously, the decrease of mitochondrial membrane potential and the opening of the mitochondrial permeability transition pore, but not ATP reduction, have been shown to be involved in rotenone-induced apoptosis (11–13). However, the role of rotenone-induced mitochondrial ROS production has not been fully investigated. Results from the current study identified mitochondrial ROS as playing a key role in rotenone-induced apoptosis.

REFERENCES

- Green, D. R., and Reed, J. C. (1998) *Science* **281**, 1309–1312
- Kroemer, G., and Reed, J. C. (2000) *Nat. Med.* **6**, 513–519
- Wang, X. (2001) *Genes Dev.* **15**, 2922–2933
- Liu, X., Kim, C. N., Yang, J., Jemmerson, R., and Wang, X. (1996) *Cell* **86**, 147–157
- Du, C., Fang, M., Li, Y., Li, L., and Wang, X. (2000) *Cell* **102**, 33–42
- Verhagen, A. M., Ekert, P. G., Pakusch, M., Silke, J., Connolly, L. M., Reid, G. E., Moritz, R. L., Simpson, R. J., and Vaux, D. L. (2000) *Cell* **102**, 43–53
- Li, L. Y., Luo, X., and Wang, X. (2001) *Nature* **412**, 95–99
- Susin, S. A., Lorenzo, H. K., Zamzami, N., Marzo, I., Snow, B. E., Brothers, G. M., Mangion, J., Jacotot, E., Costantini, P., Loeffler, M., Larochette, N., Goodlett, D. R., Aebbersold, R., Siderovski, D. P., Penninger, J. M., and Kroemer, G. (1999) *Nature* **397**, 441–446
- Reed, J. C. (1994) *J. Cell Biol.* **124**, 1–6
- Reed, J. C. (1997) *Nature* **387**, 773–776
- Barrientos, A., and Moraes, C. T. (1999) *J. Biol. Chem.* **274**, 16188–16197
- Isenberg, J. S., and Klauing, J. E. (2000) *Toxicol. Sci.* **53**, 340–351
- Chauvin, C., De Oliveira, F., Ronot, X., Mousseau, M., Lefevre, X., and Fontaine, E. (2001) *J. Biol. Chem.* **276**, 41394–41398
- Higuchi, M., Proske, R. J., and Yeh, E. T. (1998) *Oncogene* **17**, 2515–2524
- Shimizu, S., Eguchi, Y., Kamiike, W., Waguri, S., Uchiyama, Y., Matsuda, H., and Tsumimoto, Y. (1996) *Oncogene* **12**, 2045–2050
- Sherer, T. B., Betarbet, R., Stout, A. K., Lund, S., Baptista, M., Panov, A. V., Cookson, M. R., Greenamyre, J. T. (2002) *J. Neurosci.* **22**, 7006–7015
- Vrablic, A. S., Albright, C. D., Craciunescu, C. N., Salganik, R. I., and Zeisel, S. H. (2001) *FASEB J.* **15**, 1739–1744
- Torres-Roca, J. F., Tung, J. W., Greenwald, D. R., Brown, J. M., Herzenberg, L. A., Herzenberg, L. A., and Katsikis, P. D. (2000) *J. Immunol.* **165**, 4822–4830
- Deshpande, S. S., Angkeow, P., Huang, J., Ozaki, M., and Irani, K. (2000) *FASEB J.* **14**, 1705–1714
- Heussler, V. T., Fernandez, P. C., Botteron, C., and Dobbelaere, D. A. (1999) *Cell Death Differ.* **6**, 342–350
- Kelso, G. F., Porteous, C. M., Coulter, C. V., Hughes, G., Porteous, W. K., Ledgerwood, E. C., Smith, R. A., and Murphy, M. P. (2001) *J. Biol. Chem.* **276**, 4588–4596
- Koren, R., Hadari-Naor, I., Zuck, E., Rotem, C., Liberman, U. A., and Ravid, A. (2001) *Cancer Res.* **61**, 1439–1444
- Chrestensen, C. A., Starke, D. W., and Mיעyal, J. J. (2000) *J. Biol. Chem.* **275**, 26556–26565
- Gottlieb, E., Vander Heiden, M. G., and Thompson, C. B. (2000) *Mol. Cell Biol.* **20**, 5680–5689
- Garcia-Ruiz, C., Colell, A., Mari, M., Morales, A., and Fernandez-Checa, J. C. (1997) *J. Biol. Chem.* **272**, 11369–11377
- Cai, J., and Jones, D. P. (1998) *J. Biol. Chem.* **273**, 11401–11404
- Shaulian, E., Schreiber, M., Piu, F., Beeche, M., Wagner, E. F., and Karin, M. (2000) *Cell* **103**, 897–907
- Kroemer, G., Dallaporta, B., and Resche-Rigon, M. (1998) *Annu. Rev. Physiol.* **60**, 619–642
- Martinou, J. C. (1999) *Nature* **399**, 411–412
- Tan, S., Sagara, Y., Liu, Y., Maher, P., and Schubert, D. (1998) *J. Cell Biol.* **141**, 1423–1432
- Turrens, J. F., Boveris, A. (1980) *Biochem. J.* **191**, 421–427
- Turrens, J. F., Alexandre, A., and Lehninger, A. L. (1985) *Arch. Biochem. Biophys.* **237**, 408–414
- Turrens, J. F. (1997) *Biosci. Rep.* **17**, 3–8
- Cadenas, E., Boveris, A., Ragan, C. I., and Stoppani, A. O. (1977) *Arch. Biochem. Biophys.* **180**, 248–257
- Turrens, J. F., Freeman, B. A., Levitt, J. G., and Crapo, J. D. (1982) *Arch. Biochem. Biophys.* **217**, 401–410
- Nakamura, K., Bindokas, V. P., Kowlessur, D., Elas, M., Milstien, S., Marks, J. D., Halpern, H. J., and Kang, U. J. (2001) *J. Biol. Chem.* **276**, 34402–34407
- Schuchmann, S., and Heinemann, U. (2000) *Free Radic. Biol. Med.* **28**, 235–250
- Li, Y., and Trush, M. A. (1998) *Biochem. Biophys. Res. Commun.* **253**, 295–299
- Gomez-Diaz, C., Villalba, J. M., Perez-Vicente, R., Crane, F. L., Navas, P.

- (1997) *Biochem. Biophys. Res. Commun.* **234**, 79–81
40. Melendez, J. A., and Davies, K. J. A. (1996) *J. Biol. Chem.* **271**, 18898–18903
41. Rustin, P., Chretien, D., Bourgeron, T., Gerard, B., Rotig, A., Saudubray, J. M., and Munnich, A. (1994) *Clin. Chim. Acta* **228**, 35–51
42. Hansford, R. G., Hogue, B. A., and Mildaziene, V. (1997) *J. Bioenerg. Biomembr.* **29**, 89–95
43. Sohal, R. S. (1991) *Mech. Ageing Dev.* **60**, 189–198
44. Carter, W. O., Narayanan, P. K., and Robinson, J. P. (1994) *J. Leukoc. Biol.* **55**, 253–258
45. Herrmann, M., Lorenz, H. M., Voll, R., Grunke, M., Woith, W., and Kalden, J. R. (1994) *Nucleic Acids Res.* **22**, 5506–5507
46. Darzynkiewicz, Z., Li, X., and Gong, J. (1994) *Methods Cell Biol.* **41**, 15–38
47. Stefanelli, C., Bonavita, F., Stanic, I., Farruggia, G., Falcieri, E., Robuffo, I., Pignatti, C., Muscari, C., Rossoni, C., Guarnieri, C., and Caldarera, C. M. (1997) *Biochem. J.* **322**, 909–917
48. Eguchi, Y., Shimizu, S., and Tsujimoto, Y. (1997) *Cancer Res.* **57**, 1835–1840
49. Leist, M., Single, B., Castoldi, A. F., Kuhnle, S., and Nicotera, P. (1997) *J. Exp. Med.* **185**, 1481–1486
50. Sweet, S., and Singh, G. (1995) *Cancer Res.* **55**, 5164–5167
51. Freeman, B. A., and Crapo, J. D. (1982) *Lab. Invest.* **47**, 412–426
52. Boveris, A., and Cadenas, E. (1975) *FEBS Lett.* **54**, 311–314
53. Dionisi, O., Galeotti, T., Terranova, T., and Azzi A. (1975) *Biochim. Biophys. Acta* **403**, 292–300
54. Weisiger, R. A., and Fridovich, I. (1973) *J. Biol. Chem.* **248**, 3582–3592